

Active Structural Control of Impacts with a View Towards Noise Control

C. Hoever¹, W. Kropp², B.A.T. Petersson³

¹ BAM Bundesanstalt für Materialforschung und -prüfung, 12205 Berlin, Germany, Email: carsten.hoever@bam.de

² Chalmers Teknisk Högskola, 41296 Göteborg, Sweden

³ Technische Universität Berlin, 10587 Berlin, Germany

Introduction

Impacts between bodies of any sort often constitute an important source of noise and vibration. These impacts can be characterised as very short contacts between bodies leading to a sudden release of energy as audible noise and to vibrations of the involved structures. Resulting sound pressure levels often pose a serious health risk and structural vibrations lead to further noise emission, material fatigue and breakdown.

Due to a variety of source mechanisms and multiple possible ways of transmission, propagation and radiation, classical methods of noise and vibration control are often difficult to implement. In this study it is theoretically investigated how noise and vibration generated by a sphere-plate impact can be affected by application of an active force acting on the plate at the impact location.

Two different numerical models are derived as a basis for simulations. A parameter study is conducted to investigate the possibilities of active structural control of impacts. With the obtained data, an active control configuration is developed which is applicable to a wide variety of plate-sphere impact situations and which leads to promising noise and vibration reduction.

Theory

The process of a sphere impacting a simply supported plate, as depicted in Figure 1, can be divided into two individual sub-processes with their own particular sets of equations of motion (EOM). The first set describes the free fall of the sphere before and after an impact and the free vibration of the plate after the impact while the second set of EOMs models the impact process between the two bodies.

A local displacement variable ξ is defined, expressing the distance between the lowest point of the sphere ξ_s and the plate surface ξ_p (see Figure 1)

$$\xi(t) = \xi_s(t) - \xi_p(t) \quad [\text{m}] \quad (1)$$

For sphere-plate contact it is $\xi(t) \leq 0$, in this case ξ expresses the penetration depth of the sphere into the plate as shown by Figure 2. Based on $\xi(t)$ also a relative velocity $v(t)$ and acceleration $a(t)$ can be defined.

Combination of the equations of motion for plate and sphere for the contact case yields

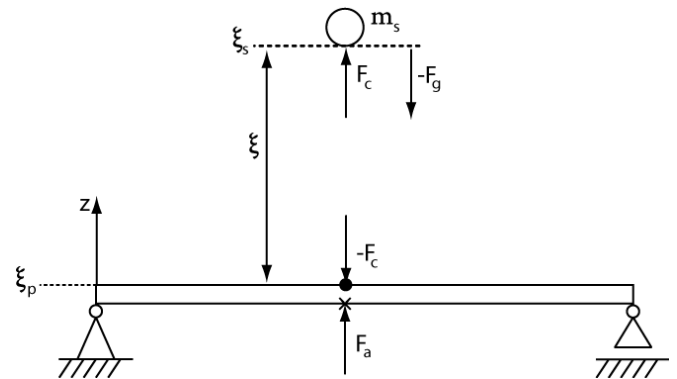


Figure 1: Side view of problem setup. Offset of forces only for visualisation. F_g denotes the gravitational force, F_c the contact force.

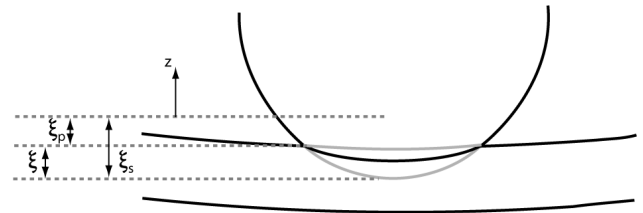


Figure 2: Deformation of plate and sphere during contact. Black: actual shape of plate and sphere during contact. Grey: Shape without deformation.

$$-m_s g - m_s a(t) + F_c(t) = -m_s F_c(t) * g_{c,a}(t) + m_s F_a(t) * g_{c,a}(t) \quad (2)$$

with $*$ denoting convolution, m_s being the mass of the sphere, g being the gravitational constant and $g_{c,a}$ the Green's function of the plate. Furthermore F_a is the active force which is applied to the plate and F_c the contact force, which is modelled according to the Hertz theory of elastic contact (see [1, 2]) as

$$F_c(t) = s (-\xi(t))^{\frac{3}{2}} \mathcal{H}\{-\xi(t)\} \quad [\text{N}] \quad (3)$$

Herein s is the Hertz contact stiffness.

In order to account for the energy loss during the impact, some form of damping has to be introduced into (1). Due to the variety of possible damping mechanisms which can occur (e.g. relaxation processes in the structures,

friction, compression of air, etc.) it is not possible to adequately cover all energy dissipation mechanisms with one single damping theory. Two different damping expressions which have been applied to impacts in the literature ([2, 3] and [4]) are evaluated, with the first being relaxation damping, giving

$$F_{c,\tau}(t) = \left[s_{rel}(-\xi(t)) - \frac{s_{\tau}}{\tau} \left((-\xi(t)) * e^{-\frac{t}{\tau}} \right) \right] \cdot \sqrt{-\xi(t)} \cdot \mathcal{H}\{-\xi(t)\}. \quad (4)$$

s_{rel} and s_{τ} are the relaxation stiffnesses for a Hertzian contact and τ is the relaxation time. Albeit relaxation gives a physically sound description of dissipation in structures, the complexity of (4) might not be well suited for numerical simulations. Due to this also a viscous damping model is investigated

$$F_{\nu}(t) = c(t) (-v(t)) \mathcal{H}\{-\xi(t)\}. \quad [\text{N}] \quad (5)$$

Herein, $c(t)$ is the viscous damping factor.

Simulations

A numerical impact simulation can be performed by introducing (4) respectively (5) into (2), subsequent discretisation and application of the Newton-Raphson (see [5]) and Hilber-Hughes-Taylor methods (see [6]).

Considered is the impact of a steel sphere of radius $R = 0.02$ m onto a simply supported quadratic aluminium plate of $0.5 \text{ m} \times 0.5 \text{ m}$ with the impact position being exactly in the middle of the plate.

Simulations are performed by adjusting the damping parameters of equations (4) and (5) to give an initial rebound height which is in accordance with a coefficient of restitution $cor = 0.7$ as found in the literature (see [1, 4]).

Comparison of Damping Models

Before investigating the influence of the active force on the impact process, the implemented numerical simulation of the sphere falling onto the plate as such is investigated. This is done to ensure a correct simulation of the physical process and to assess the applicability of the two employed damping methods.

The rebound sequence is shown in Figure 3. It can be seen that for impacts following the first one the rebound heights for both methods do not reach the values expected from the cor . While deviations can be considered acceptable for viscous damping, this is not the case for relaxation damping which actually shows one rebound less than the viscous case.

Further observations regarding the behaviour of both methods can be found in Table 1. It can be seen that even though the viscous model is physically more abstract, it actually gives better results than relaxation damping.

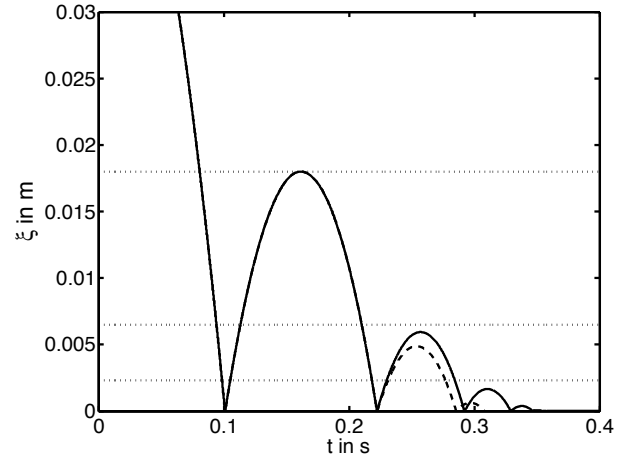


Figure 3: Comparison of relaxation and viscous damping simulations. Initial height 0.05 cm at $t = 0$ s. (---) relaxation, (—) viscous damping, (···) expected rebound heights according to cor .

	Relaxation	Viscous
Physical adequacy	good	limited
Successive rebound simulation	not satisfying	ok
Damping parameters	s_{rel}, s_{τ}, τ	c
Numerical solving		
Discretised equations	complex	simple
Average iterations	≈ 2800	2
Convergence	$< 100\%$	100%

Table 1: Comparison of simulation performance for relaxation and viscous damping.

It is believed that this can partly be attributed to the complexity of the relaxation formulation (4), which seems to cause numerical problems. Problematic is also the adjustment of s_{rel} , s_{τ} and τ for which it is difficult to find reference data. In this regard the viscous model — with just one parameter (c) to adjust — seems less error prone. Taking all this into consideration, it is believed that viscous damping is the more suitable tool for the requirements of this study and will be used for all following calculations.

Parameter Study

The acoustically relevant quantities of an impact are:

1. Acceleration noise (E_{Acc}, p_{max}),
2. plate vibrations ($E_{vib}, v_{p,max}$),
3. ringing noise (E_{rad} in audible range)
4. and rebound height (ξ_{reb}).

The rebound height is included as it determines the impact velocity for a successive impact during a free fall situation. Different active control schemes are possible, depending on whether it is aimed for reduction of an individual quantities, a group of quantities or all of them.

Due to the complexity of the governing equations and the variety of the relevant quantities it is difficult to

Quantity	max. Reduct.	Configuration	Side effect
E_{Acc}	-11 dB	$F_{cos,1}$ $t_a = 11, \kappa = -1.5$	$E_{vib} = +2$ dB $v_{p,max} = +3$ dB
p_{max}	-2 dB	$F_{cos,1}$ $t_a = 11, \kappa = -1.5$	$E_{vib} = +2$ dB $v_{p,max} = +3$ dB
E'_{vib}	-3 dB	$F_{c,1}$ $t_a = 11, \kappa = 0.8$	-
$v'_{p,max}$	-3 dB	$F_{cos,2}$ $t_a = 1, \kappa = -0.4$	-
E'_{rad}	-5 dB	$F_{c,2}$ $t_a = 11, \kappa = 1.0$	-
ξ'_{reb}	8 %	$F_{sin,1}$ $t_a = 1, \kappa = -1.0$	$v_{p,max} = 4$ dB $E_{vib} = 1$ dB
v'_{next}	8 %	$F_{sin,1}$ $t_a = 1, \kappa = -1.0$	$v_{p,max} = 4$ dB $E_{vib} = 1$ dB

Table 2: Maximum reduction of noise and vibration quantities obtained during the parameter study. t_a is the time step of the impact at which F_a starts to act, κ the scaling factor compared to $F_{c,0}$.

directly derive optimal force configurations from the mathematical description of the impact. Hence, a parameter study is conducted to assess the general influence of active control forces of different shape and strength. In the following section it is then investigated how the results of the parameter study can be applied to a wide variety of real impacts with different configurations.

Regarding amplitude and/or shape, all investigated active forces are based on the contact force without active control $F_{c,0}$. The following configurations for F_a are examined:

1. Differently scaled constant values,
2. scaled and/or time shifted versions of $F_{c,0}$,
3. scaled and/or time shifted sines based on $F_{c,0}$,
4. scaled and/or time shifted cosines based on $F_{c,0}$.

Information about the maximum reduction which is obtained during the parameter study can be found in Table 2. Without going into details it can be seen that the individual quantities can be reduced by a considerable amount. As expected, maximum reduction is not achieved with the same active force configuration for all quantities, instead there are five different configurations for the seven quantities. Moreover, in four cases a side effect can be found, i.e. maximum reduction of one quantity leads to an impairment of another one. On the other hand, three configurations do not show any impairment at all, making them promising candidates for further investigation.

In Figure 4 one of the three active force configurations is shown exemplarily. Generally, some common features can be deduced from the three configurations leading to optimisation without side effects:

1. Amplitude is lower than $\max(F_{c,0})$,
2. directed upwards,

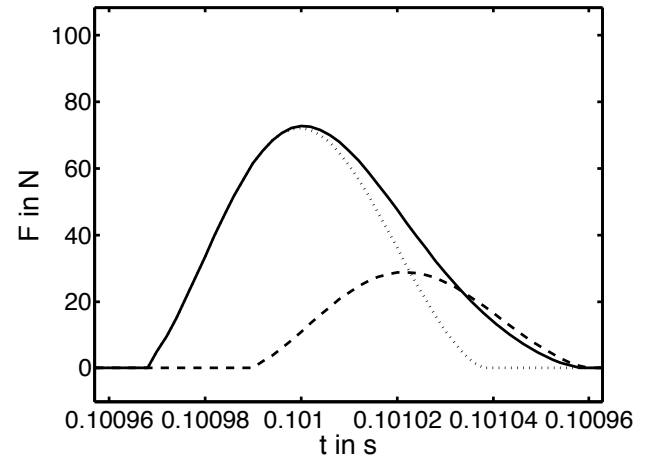


Figure 4: Example of an optimum active force configuration ($F_{c,1}$) for single parameter reduction for first impact on aluminium plate. (\cdots) contact force for case without active control, ($- -$) applied active force, ($-$) resulting contact force for applied active force.

3. start slightly before max. deformation is reached,
4. fade in and fade out smoothly
5. and application for a slightly longer period of time than an uncontrolled impact.

Physically this can be interpreted as follows: The aim is to maximise the amount of energy transferred to the local deformation of plate and sphere without actively pushing the sphere upwards or exciting the plate with the active force.

Development of an Active Control Method

The results of the parameter study are based on artificial conditions which are unlikely to be met for real impacts. Especially problematic is the dependance on parameters based on $F_{c,0}$. Hence, while the proceedings of the parameter study are useful for a general evaluation of possible force configurations and lead to valuable results, a practical implementation has to be realised differently, using universal parameters which are independent of any a priori knowledge about the impact conditions.

The parameters should be sufficiently precise, applicable to a broad range of impact conditions and not too complex to implement. The last condition is based on the circumstance that the usually very short contact times do not allow for complicated calculations with long execution times.

In this context, it is helpful that the findings of the parameter study reveal that promising results are mostly obtained when there is a time delay between the beginning of the contact and the start of the active force. This allows the replacement of the time delay t_a with a control variable based on the slope of $\xi(t)$ respectively $F_c(t)$. For the deformation the following can be applied: From the beginning of the contact the penetration depths are

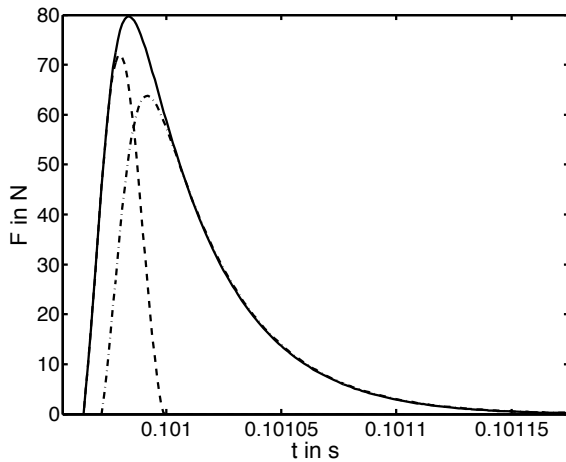


Figure 5: Forces for the first impact on the aluminium plate with an optimised active force configuration. Drop height 0.05 m. (—) impact without active control, (---) impact with active force, (- · -) applied active force ($\kappa = 0.8$, $v_{thr} = -0.25$ m/s).

detected and stored at specific time samples, i.e. $\xi(t_N)$. This allows estimation of the slope as

$$v(t) \approx \frac{\xi(t_N) - \xi(t_{N-1})}{\Delta t}. \quad [\text{m/s}] \quad (6)$$

For the impacting part of the contact where no active force acts, a specific slope can unambiguously be connected to a time delay which is related to the length of the contact without active control. Hence, the time delay is no longer specified in absolute values (i.e. time steps or seconds) but as a slope, or equivalently impact velocity, threshold v_{thr} .

The active force starts to act as soon as the slope (which is negative during the first part of the impact) gets higher than v_{thr} . Based on the findings of the previous section, the active force is then applied as a shifted and scaled version of the contact force which is calculated from the real penetration depth:

$$F_a = \kappa \cdot \{-\xi(t - t_a)\}^{\frac{3}{2}} s. \quad [\text{N}] \quad (7)$$

where t_a is now specified by the time delay between the start of the contact and the moment where v_{thr} is reached. Apart from the simplicity of implementation and the universal applicability, this approach has another advantageous feature. By defining F_a based on values of ξ given by the actual contact, any influence of the active force at time t also propagates to a later time $t + t_a$ where F_a is based on $\xi(t)$.

For reasonable force configurations this automatically leads to an extension of F_a with a decreased slope, see Figure 5. The previous section has shown that this is a most expedient behaviour. Compared to Table 2 further reductions in the range of -1 dB to more than -30 dB

can be achieved. The general results are comparable for a broad range of different impact conditions (materials, initial impact height, etc.), meaning the proposed approach is not limited to the conditions of the parameter study but applicable to a variety of different impact conditions.

Concluding Remarks

The most important remarks related to the numerical simulations are the shortcomings associated with the implemented relaxation model. The problems related to the Newton-Raphson root finding — erratic convergence behaviour and partly low execution speed — prevent examination of some configurations. This problem is, at least partly, believed to be related to the enhanced complexity of the numerical equations. Adding the complexity and uncertainty introduced by the replacement of the Hertz' stiffness s with the relaxation parameter s_{rel} , s_τ and τ , it is obvious why the implementation of a different damping model is deemed necessary in this study.

Within the limits of the desired application the viscous damping model proves to be a tool fulfilling all requirements. It is numerically very efficient, comparably easy to implement and gives satisfying results.

Regarding the actual task of developing an active control scheme for impact related noise and vibrations results have been obtained which show that all relevant noise and vibration quantities can individually be optimised by proper force configurations. Furthermore, certain force configurations lead to optimisation of all quantities.

Finally, an implementation of an active control scheme without a priori knowledge about the impact conditions is theoretically feasible. It is believed that the presented active control method can be successfully applied in practice. The biggest problem for real application is seen in the circumstance that impact detection and application of F_a are restrained to the actual impact location. This puts high demands on the actual setup and limits the choice of equipment for sensor and actuator.

References

- [1] Impact. Goldsmith, London, 1960
- [2] Contact mechanics. Johnson, Cambridge, 1987
- [3] Development and primary investigation of a code to simulate non-linear-plate impact interaction. Späh, Chalmers University of Technology, 2007
- [4] Mechanical Impact Dynamics. Brach, New York, 1991
- [5] Numerical Recipes in C — The Art of Scientific Computing, 2nd edition. Press et al., Cambridge, 1992
- [6] Extensions of the HHT- α method to differential-algebraic equations in mechanics. Electronic Transactions on Numerical Analysis **26** (2007), 190-208